

Analog computing using graphene-based metalines

SAJJAD ABDOLLAHRAMEZANI, KAMALODIN ARIK, AMIN KHAVASI,* AND ZAHRA KAVEHVASH

Department of Electrical Engineering, Sharif University of Technology, P.O. Box 11555-4363, Tehran, Iran

*Corresponding author: khavasi@sharif.edu

Received 8 September 2015; revised 16 October 2015; accepted 16 October 2015; posted 16 October 2015 (Doc. ID 249647); published 5 November 2015

We introduce the new concept of “metalines” for manipulating the amplitude and phase profile of an incident wave locally and independently. Thanks to the highly confined graphene plasmons, a transmit-array of graphene-based metalines is used to realize analog computing on an ultra-compact, integrable, and planar platform. By employing the general concepts of spatial Fourier transformation, a well-designed structure of such meta-transmit-array, combined with graded index (GRIN) lenses, can perform two mathematical operations, i.e., differentiation and integration, with high efficiency. The presented configuration is about 60 times shorter than the recent structure proposed by Silva *et al.* [Science 343, 160 (2014)]; moreover, our simulated output responses are in better agreement with the desired analytical results. These findings may lead to remarkable achievements in light-based plasmonic signal processors at nanoscale, instead of their bulky conventional dielectric lens-based counterparts. © 2015 Optical Society of America

OCIS codes: (070.1170) Analog optical signal processing; (250.5403) Plasmonics; (130.3120) Integrated optics devices.

<http://dx.doi.org/10.1364/OL.40.005239>

Recently, realization of analog computing has been achieved by manipulating continuous values of phase and amplitude of the transmitted and reflected waves by means of artificial engineered materials, known as metamaterials, and planar easy-to-fabricate metamaterials with periodic arrays of scatterers, known as metasurfaces [1–3]. Both above-mentioned platforms offer the possibility of miniaturized wave-based computing systems that are several orders of magnitude thinner than conventional bulky lens-based optical processors [1,4].

Challenges associated with the complex fabrication of metamaterials [5] besides absorption loss of the metal constituent of metasurfaces [6,7] degrade the quality of practical applications of relevant devices. As a result, graphene plasmonics can be a promising alternative due to the tunable conductivity of graphene and highly confined surface waves on graphene, the so-called graphene plasmons (GPs) [8,9].

We present a planar graphene-based configuration for manipulating GP waves to perform desired mathematical operations

at nanoscale. By applying appropriate external gate voltage and a well-designed ground plane thickness profile beneath the dielectric spacer holding the graphene layer, desired surface conductivity values are achieved at different segments of the graphene layer [8]. To illustrate the applications of the proposed configuration, two analog operators, i.e., differentiator and integrator, are designed and realized. The proposed structure will be two-dimensional (2D) which is an advantage compared to the previously reported three dimensional structures [1–3] that manipulate one-dimensional (1D) variable functions.

We introduce a new class of meta-transmit-arrays (MTA) based on graphene: metalines which are 1D counterparts of metasurfaces. Our approach for realizing mathematical operators is similar to the first approach of [1]: i.e., metaline building blocks (instead of metasurfaces) perform mathematical operations in the spatial Fourier domain. However, the main advantage of our structure is that it is ultra-compact (its length is about $1/60$ of the free space wavelength, λ) in comparison with the structure proposed by Silva *et al.* whose length is about $\lambda/3$ [1]. It should also be noted that, in this Letter, the whole structure (including lenses and metalines) is implemented on graphene. Therefore, the total length of the proposed device is about $\lambda/4$, about 60 times shorter than the one reported in [1].

The general concept of performing a mathematical operation in the spatial Fourier domain is graphically shown in Fig. 1(a). In this figure, z is the propagation direction, $b(x, y)$ indicates the desired 2D impulse response, $f(x, y)$ is an arbitrary input function, and $g(x, y)$ describes the corresponding output function. The whole system is assumed to be linear transversely invariant and, thus, the input and output functions are related to each other via the linear convolution [2]:

$$\begin{aligned} g(x, y) &= b(x, y) * f(x, y) \\ &= \iint b(x - x', y - y') f(x', y') dx' dy'. \end{aligned} \quad (1)$$

Transforming Eq. (1) to the spatial Fourier domain leads to

$$G(k_x, k_y) = H(k_x, k_y) F(k_x, k_y), \quad (2)$$

where $G(k_x, k_y)$, $H(k_x, k_y)$, and $F(k_x, k_y)$ are the Fourier transforms of their counterparts in Eq. (1), respectively, and (k_x, k_y) denotes the 2D spatial Fourier domain variables.

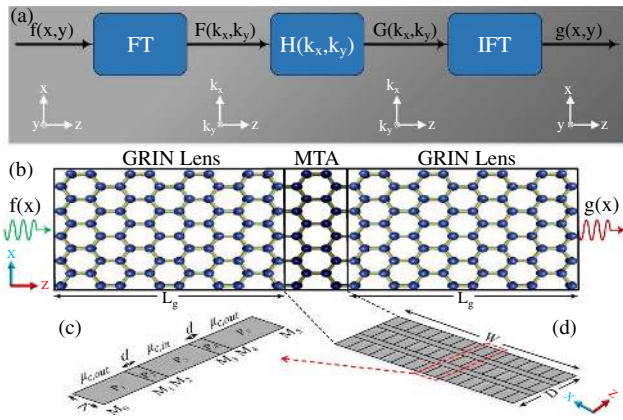


Fig. 1. (a) Sketch of linear transversely invariant system to perform mathematical operations. (b) Schematic of 2D graphene-based computing system. (c) Basic building block of the metalines labeled by the propagation and matching matrices corresponding to the interfaces and segments. (d) Sketch of the meta-transmit-array made of three symmetric stacked metalines. The dimensions are $W = 684$ nm, $L_g = 1028$ nm, $D = 100$ nm, $\Lambda = 18$ nm, $d = 5$ nm, and $\lambda = 6$ μ m.

For our 2D graphene-based system, as shown in Fig. 1(b), the above formulation is sufficient to be presented in one dimension. In this figure, $f(x)$ and $g(x)$ represent the transverse field distribution of the incident and transmitted waves, and $H(k_x)$ is the appropriate transfer function. Accordingly, Eq. (2) can be interpreted as $g(x) = \text{IFT}\{H(k_x)\text{FT}[f(x)]\}$, where (I)FT means (inverse) Fourier transform. The transfer function is given in the spatial Fourier domain k_x ; on the other hand, the incident wave ($f(x)$) is also transformed into the Fourier domain. Hence, any transfer function can be realized by properly manipulating the Fourier-transformed wave in its transverse direction x [1]. Fourier transform can be carried out by a lens at its focal point while realizing inverse Fourier transform with real materials is not possible thus, instead, we employ the relation $g(-x) = \text{FT}\{H(k_x)\text{FT}[f(x)]\}$. This relation can be easily obtained from the well-known formula $\text{FT}\{\text{FT}[g(x)]\} \propto g(-x)$ and implies that the output will be proportional to the mirror image of the desired output function $g(x)$ [1].

For performing Fourier transform, we use graded index (GRIN) lenses. Since the optical properties of dielectric GRIN lenses change gradually, the scattering of the wave could be significantly reduced which leads to higher efficiency. To realize the graphene-based type of such lenses, the surface conductivity of graphene should be properly patterned in a way that the effective mode index of GP waves follows the quadratic refractive index distribution of their dielectric counterparts [10].

In this Letter, we implement the appropriate transfer function $H(k_x)$ by means of a new type of MTA on graphene. To manipulate the transmitted wave efficiently, not only should the transmission amplitude be completely controlled in the range of 0–1, but also the transmission phase should cover the whole 2π range independently [11]. To this end, similar to the approach of Monticone *et al.* [4], a meta-transmit-array comprised of symmetric stack of three metalines separated by a quarter-guided wavelength transmission line is utilized [Fig. 1(d)] in which each unit cell operates as a nanoscale spatial light modulator [Fig. 1(c)]. To simplify the design procedure,

the two outer stacks are chosen to be identical, but different from the inner one.

To fully control the transmission phase, in addition to amplitude, we need to locally manipulate propagating GP waves along and across the meta-transmit-array [4]. As described previously, this GP surface wave engineering is achieved via surface conductivity variation through an uneven ground plane beneath the graphene layer.

Recently, analytical results for the reflection and transmission coefficients of GP waves at 1D surface conductivity discontinuity have been reported [12]:

$$r_{LR} = e^{i\vartheta_{LR}} \frac{k_L - k_R}{k_L + k_R}, \quad t_{LR} = \frac{2(k_L k_R)^{1/2}}{k_L + k_R}, \quad (3)$$

where

$$\vartheta_{LR} = 2\Psi(-k_L) = \frac{\pi}{4} - \frac{2}{\pi} \int_0^\infty \frac{\arctan(k_L u / k_R)}{u^2 + 1} du. \quad (4)$$

In these equations, $k_{L,R} = 2i\omega\epsilon_e/\sigma_{L,R}$ are the GP wavenumbers of left and right side regions of the discontinuity in the quasi-static approximation, while $\sigma_{L,R}$ represent their corresponding complex surface conductivities and ϵ_e is the average permittivity of the upper and lower media surrounding the graphene sheet. Similarly, for a GP wave incident on the discontinuity from the right side region, the coefficients r_{RL} and t_{RL} can be simply achieved by exchanging k_L and k_R in Eqs. (3) and (4).

To relate the forward-backward fields on one side of the interface to those on the other side, the matching matrix is applied. The matching matrix of the interface achieved by employing the reciprocity theorem and the propagation matrix, which relates propagative forward-backward fields along a segment, is obtained as follows [13]:

$$M_m = \begin{pmatrix} r_{LR,m} & t_{RL,m} \\ t_{LR,m} & r_{RL,m} \end{pmatrix}, \quad P_n = \begin{pmatrix} e^{-ik_n l_n} & 0 \\ 0 & e^{ik_n l_n} \end{pmatrix}, \quad (5)$$

where $m = 0, \dots, 5$ is the m th interface of the building block; and $n = 1, \dots, 5$ is the n th segment of the unit cell [see Fig. 1(c)]. Finally, the scattering parameters can be easily calculated using the whole building block transfer matrix obtained by multiplication of the matching and propagation matrices [13]:

$$T = M_0 \prod_{k=1}^5 P_k M_k. \quad (6)$$

The amplitude and phase of S_{21} versus the chemical potentials of the inner and outer metalines, $\mu_{c,in}$ and $\mu_{c,out}$, are plotted in Figs. 2(a) and 2(b), calculated by means of our analytical approach. It is obvious that by local tuning of the chemical potential of each unit cell any transmission phase and amplitude profile can be achieved.

Now, we implement first differentiation, second differentiation, and integration operators with the proposed structure. It is well known that the n th derivative of a function is related to its first Fourier transform by $d^n(f(x))/dx^n = F^{-1}\{(ik_x)^n F(f(x))\}$. Obviously, to realize the n th derivation we have to perform a transfer function of $(ik_x)^n$. Thus, as described in the previous section, we set the transfer function of the meta-transmit-array to $H(x) \propto (ix)^n$. Since metalines are inherently passive media, the desired transfer function has to be normalized to the lateral limit to ensure unity across the structure the maximum transmittance; thus, the appropriate transfer function is $H(x) \propto (ix/(W/2))^n$. Figures 3(b) and 3(c) indicate

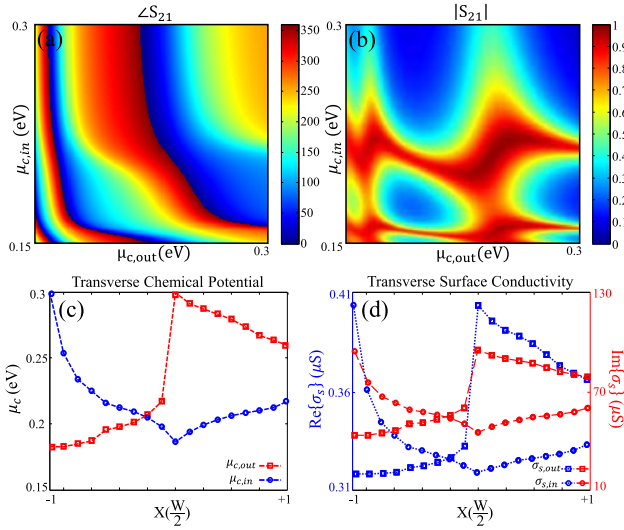


Fig. 2. (a) Phase and (b) amplitude of transmission coefficient versus the internal and external metalines' chemical potentials, $\mu_{c,in}$ and $\mu_{c,out}$, calculated by the proposed analytical approach. (c) Transverse distribution of chemical potential for the designed first-order differentiator meta-transmit-array. (d) Corresponding complex surface conductivity. The complex surface conductivity of graphene can be retrieved by the Kubo's formula [8] with $T = 300$ K and $\tau = 1$ ps.

the desired magnitude and phase profile of the first-order derivative transfer function $H(x)$. According to Figs. 2(a) and 2(b), by properly tailoring the values of the chemical potential along the lateral dimension for internal and external metalines, the transverse amplitude and phase distribution of the transfer function are implemented. To this end, the transverse distribution of chemical potential for the designed first-order differentiator meta-transmit-array and its corresponding complex surface conductivity profile are depicted in Figs. 2(c) and 2(d). Now, a TM-polarized GP surface wave is launched toward the designed meta-transmit-array, and the calculated electric field distribution is shown in Fig. 3(a), using Ansoft's HFSS. As depicted in Figs. 3(b) and 3(c), the output profile of meta-transmit-array is in excellent agreement with the desired transfer function. To be more precise, the standard deviation from the amplitude and phase of the desired transfer function is 0.04° and 6° , respectively. This is smaller than the standard deviation observed in Fig. (S7b) of [1] which is about 0.19° and 15° for the amplitude and phase, respectively. Other operators can be designed in a similar manner. To perform the second-order spatial derivative, the desired transfer function is $H(x) \propto -(x/(W/2))^2$. Although here the amplitude is a quadratic function of transverse dimension, the phase is constant. The results for the designed second-order differentiator are illustrated in Figs. 3(d)–3(f). To realize a second-order integrator, a challenge should be overcome. In this case, the desirable transfer function should be $H(x) \propto (ix)^{-2}$ which leads to an amplitude profile with values tending to infinity in the vicinity of $x = 0$. To overcome this problem, we use the following approximate transfer function [1]:

$$H(x) = \begin{cases} 1, & \text{if } |x| < b \\ (ix)^{-2}, & \text{if } |x| > b \end{cases} \quad (7)$$

where b is an arbitrary parameter that we set it to $b = W/12$. For all the points within $|x| < b$, the amplitude is assumed to be

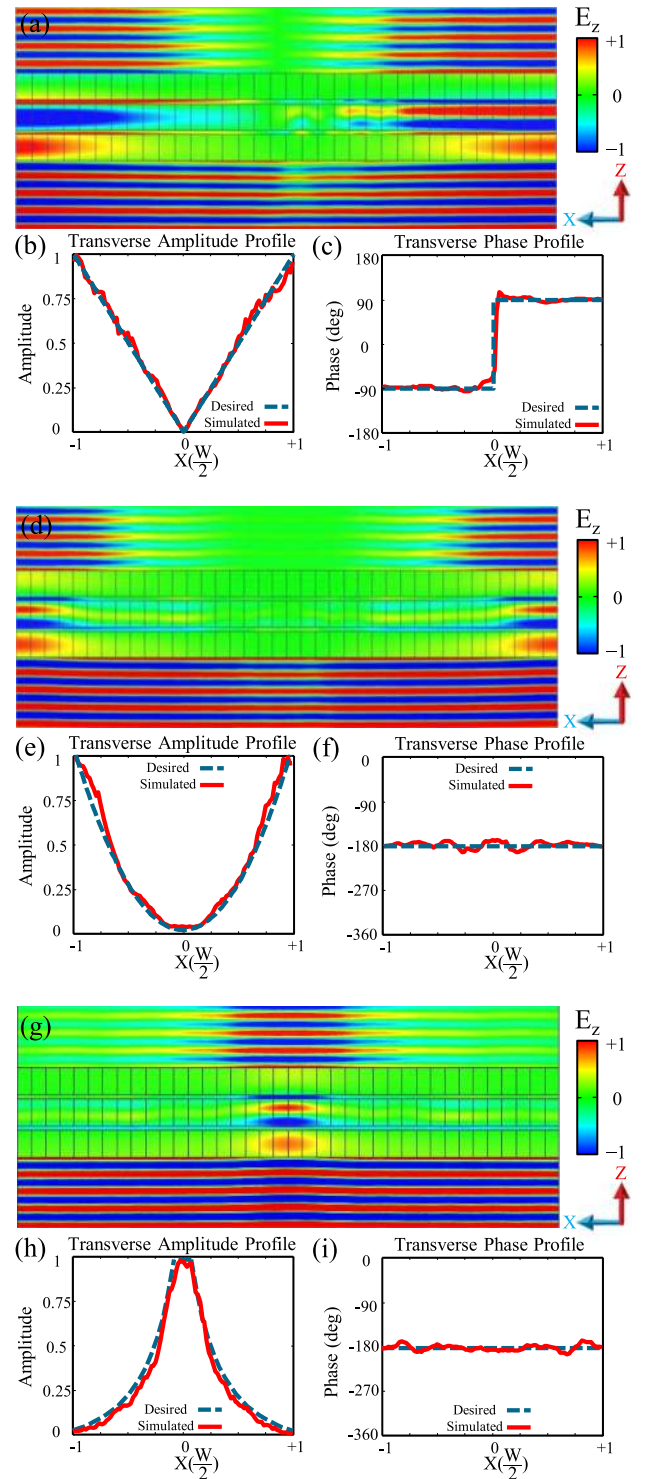


Fig. 3. (a), (d), (g) Snapshots of electric field distribution (E_z) for a TM-polarized GP surface wave incident on the designed first-order differentiator, second-order differentiator, and second-order integrator, respectively. Comparison of the corresponding transverse (b), (e), (h), amplitude and (c), (f), (i) phase distribution of transmitted wave and desired transfer function response right behind the structure.

unity; others follow the correct transfer function profile precisely. Figure 3(g) shows numerical simulation of electric field distribution for this case. By comparing the obtained results from

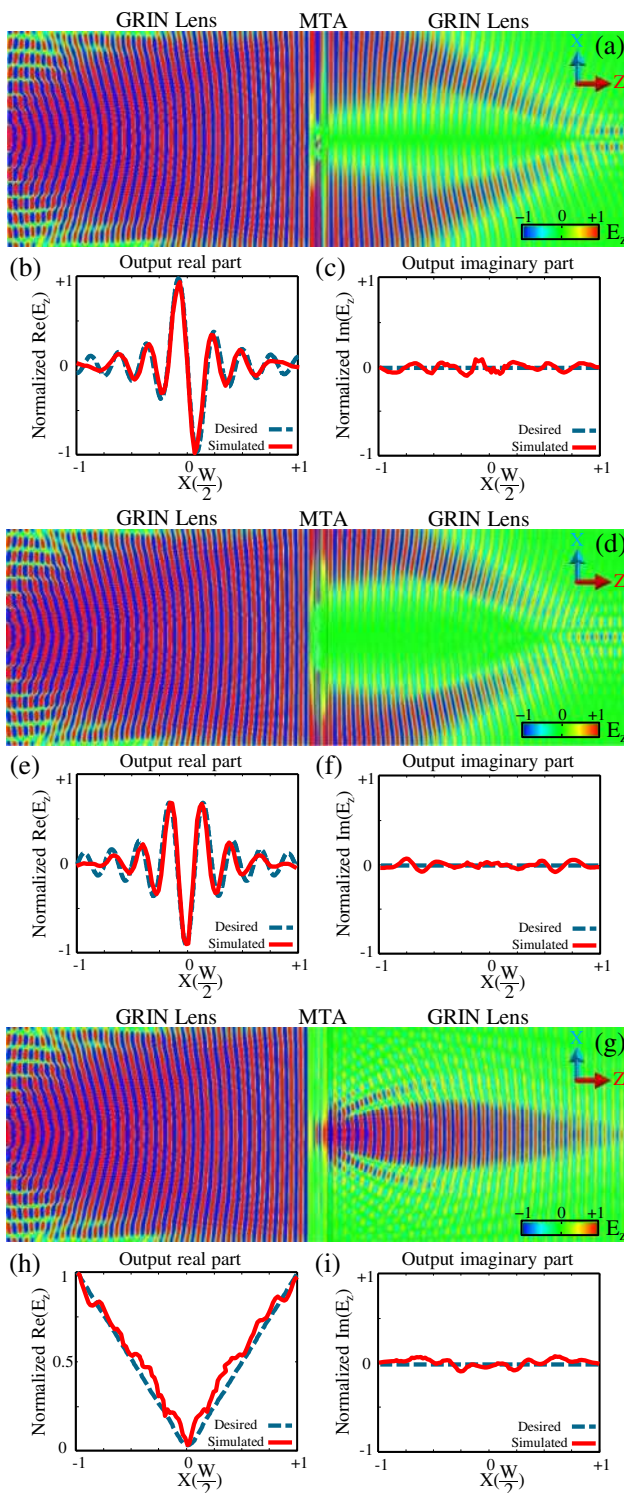


Fig. 4. (a), (d), (g) Snapshots of the z -component of the electric field distribution along the GRIN Lens/MTA/GRIN Lens for the first-order differentiator, second-order differentiator, and second-order integrator, respectively. Corresponding (b), (e), (h) real and (c), (f), (i) imaginary parts of the output electric field compared with the analytical results. The input function is $f(x) = \text{sinc}(16\pi x/W)$.

meta-transmit-array and analytical solution in Figs. 3(h) and 3(i), excellent agreement is observed. The standard deviations from the amplitude and phase of the desired transfer function of second-order differentiator and second-order integrator are $(0.09, 11^\circ)$ and $(0.09, 10^\circ)$, respectively. To demonstrate the functionality of our proposed structures, a GP surface wave in the form of a Sinc function is sourced into our proposed GRIN/meta-transmit-array/GRIN configuration and the simulated electric field distributions are illustrated in Fig. 4 for the designed first-order derivative, second-order derivative, and second-order integrator, respectively. It is obvious from these figures that the achieved results are closely proportional to the desired results calculated analytically.

In summary, we have proposed and designed a new class of planar meta-transmit-array consisting of symmetric three-stacked graphene-based metalines to perform wave-based analog computing. Using analytical results for the reflection and transmission coefficients of graphene plasmon waves at 1D surface conductivity discontinuity [12], we have demonstrated that full control over the transmission amplitude and phase can be achieved by appropriately tailoring of surface conductivity of each building block. Employing the general concept of performing mathematical operations in spatial Fourier domain, we assign the meta-transmit-array a specific transfer function corresponding to the desired operation. The two designed operators in this Letter, i.e., differentiator and integrator, illustrate a high efficiency. The proposed graphene-based structure is not only ultra-compact, but also depicts more accurate responses than the bulky structure suggested in [1]. These features are due to exceptionally high confinement of surface plasmons propagating on a graphene sheet. However, this miniature size comes at a price, namely any future fabrication imperfections and tolerance will lead to distortion of the anticipated results and, therefore, degrade the efficiency of the proposed structure. The presented approach may broaden horizons to achieve more complex nanoscale signal processors.

REFERENCES

1. A. Silva, F. Monticone, G. Castaldi, V. Galdi, A. Alù, and N. Engheta, *Science* **343**, 160 (2014).
2. A. Pors, M. G. Nielsen, and S. I. Bozhevolnyi, *Nano Lett.* **15**, 791 (2015).
3. M. Farmahini-Farahani, J. Cheng, and H. Mosallaei, *J. Opt. Soc. Am. B* **30**, 2365 (2013).
4. F. Monticone, N. M. Estakhri, and A. Alù, *Phys. Rev. Lett.* **110**, 203903 (2013).
5. F. Monticone and A. Alu, *Chin. Phys. B* **23**, 047809 (2014).
6. A. V. Kildishev, A. Boltasseva, and V. M. Shalaev, *Science* **339**, 1232009 (2013).
7. F. Aieta, P. Genevet, M. A. Kats, N. Yu, R. Blanchard, Z. Gaburro, and F. Capasso, *Nano Lett.* **12**, 4932 (2012).
8. A. Vakil and N. Engheta, *Science* **332**, 1291 (2011).
9. W. B. Lu, W. Zhu, H. J. Xu, Z. H. Ni, Z. G. Dong, and T. J. Cui, *Opt. Express* **21**, 10475 (2013).
10. G. Wang, X. Liu, H. Lu, and C. Zeng, *Sci. Rep.* **4**, 4073 (2014).
11. J. Cheng and H. Mosallaei, *Opt. Lett.* **39**, 2719 (2014).
12. B. Rejaei and A. Khavasi, *J. Opt.* **17**, 075002 (2015).
13. S. J. Orfanidis, *Electromagnetic Waves and Antennas* (Rutgers University, 2002).